Thick c-BN films deposited by radio frequency magnetron sputtering in argon/nitrogen gas mixture with additional hydrogen gas*

Yan Zhao(赵艳)[1], Wei Gao(高伟)[1], Bo Xu(徐博)[2], Ying-Ai Li(李英爱)[1], Hong-Dong Li(李红东)[1], Guang-Rui Gu(顾广瑞)[2], and Hong Yin(殷红)[1,†]

[1] *State Key Laboratory of Superhard Materials, Jilin University, Changchun* 130012, *China*
[2] *Department of Physics, College of Science, Yanbian University, Yanji* 133002, *China*

(Received 16 March 2016; revised manuscript received 23 May 2016; published online 25 Auguat 2016)

The excellent physical and chemical properties of cubic boron nitride (c-BN) film make it a promising candidate for various industry applications. However, the c-BN film thickness restricts its practical applications in many cases. Thus, it is indispensable to develop an economic, simple and environment-friend way to synthesize high-quality thick, stable c-BN films. High-cubic-content BN films are prepared on silicon (100) substrates by radio frequency (RF) magnetron sputtering from an h-BN target at low substrate temperature. Adhesions of the c-BN films are greatly improved by adding hydrogen to the argon/nitrogen gas mixture, allowing the deposition of a film up to 5-μm thick. The compositions and the microstructure morphologies of the c-BN films grown at different substrate temperatures are systematically investigated with respect to the ratio of H_2 gas content to total working gas. In addition, a primary mechanism for the deposition of thick c-BN film is proposed.

Keywords: cubic boron nitride, hydrogen plasmas, RF magnetron sputtering, growth diagram

PACS: 68.55.A–, 81.15.Cd, 68.35.B– **DOI:** 10.1088/1674-1056/25/10/106801

1. Introduction

As an analog of diamond, cubic boron nitride (c-BN) exhibits many similar outstanding properties such as extreme hardness, wide band gap, negative electron affinity, high thermal conductivity, etc.[1–12] Furthermore, c-BN also holds numerous physical properties and chemical inertness, making it more superior to diamond for future technical applications. However, the nucleation and growth of c-BN film require the high-energy ion bombardment on the growing surface no matter whether physical vapor deposition (PVD) or chemical vapor deposition (CVD) method is used, resulting in accumulation of the compressive stress.[13–17] The film thickness is usually limited up to 200 nm with poor adhesion, and this thickness is certainly not sufficient for industry applications. Thus, it is indispensable to develop an economic, simple and environment-friend method to synthesize high quality thick, stable c-BN films.

So far only a few groups have reported the synthesis of c-BN films thicker than 1 μm by using sputter and CVD methods.[18–21] Especially, with recent CVD techniques through utilizing fluorine chemistry, 20-μm-thick c-BN coatings have been achieved, which is a record thickness. In addition, heteroepitaxial c-BN films with very low compressive stress can be prepared on (001)-oriented diamond films by using ion-beam-assisted deposition.[22] However, very high temperatures up to 1000 °C are necessary for these deposition methods,[22,23] which is hence incompatible with many substrate materials. Thick c-BN coatings with drastically reduced compressive stress have been synthesized when adding oxygen gas into the sputtering gases following a gradient B–C–N layer on the substrates.[24–26] Adding a small amount of Si into c-BN films has been observed to be effective to reduce the stress as well as the resistance.[27,28] Recently, it was suggested that adding 25% hydrogen into the reactive gases would reduce the compressive stress.[29–32] Combining with a nanocrystalline diamond (NCD) as the gradient layer from Si substrate, 3-μm-thick c-BN films have been deposited by an unbalanced magnetron sputtering method.[33] Theoretical and experimental studies demonstrated that the incorporation of hydrogen into the reactive working plasma is known to preferentially stabilize the cubic structure of BN on the edges of h-BN in the CVD process.[34–36] The involvement of hydrogen is believed to inhibit the penetration of Ar into the space of (0002) h-BN planes, which is considered to be one of the major reasons for the existence of compressive stress in the magnetron sputtering procedure.[37]

Here, we will report on the deposition of high-quality c-BN thick films on Si substrates without any gradient layers by using the RF magnetron sputter method through adding

*Project supported by the National Natural Science Foundation of China (Grant Nos. 51572105, 61504046, and 51272224), the Scientific Research Foundation for the Returned Overseas Chinese Scholars, State Education Ministry, China, the Development and Reform Commission of Jilin Province, China (Grant No. 2015Y050), and the Scientific Research Foundation for the Returned Overseas of Jilin Province, China.

†Corresponding author. E-mail: hyin@jlu.edu.cn

© 2016 Chinese Physical Society and IOP Publishing Ltd

hydrogen gas into reactive gases. In the deposition process, a negative bias voltage is usually utilized to enforce the ion bombardment needed for nucleation of the cubic phase. The threshold of bias voltage ranges differently according to the growth technique, but in general it is over a hundred volts. Presently, it is expected to lower the threshold of bias voltage by the addition of hydrogen gas. An important aspect, previously overlooked in the deposition process of c-BN film, is the optimization of the experimental parameters using hydrogen gas. In this paper, firstly, we focus on the characterizations of the c-BN films prepared using H_2/Ar/N_2 mixture gases under different conditions. In addition, the parameter space is involved with samples prepared in pure Ar/N_2 mixture plasma. The high cubic content c-BN growth window is obtained in the case of using H_2 gas. The utilization of H_2 in addition to Ar/N_2 reactive gases results in much reduced compressive stress, and hence far improved adhesion.

2. Experimental details

The c-BN films were deposited on silicon substrates using the RF magnetron sputtering method. Double-side polished, (100)-oriented single-crystalline silicon (phosphor-doped, 4.5 Ω·cm, 300-μm thick) was used as the substrate material. A hexagonal BN target (pure 99.999%, 5-mm thick, 50 mm in diameter) was mounted on a water-cooled magnetron gun that was coupled with an RF (13.56 MHz) generator via a matching network. The target was sputter-cleaned for 5 min before each deposition. The substrate holder, distant 50 mm away from target, could be heated by a resistive heater and biased with a direct current (DC) power supply. The RF power applied to the target was kept constant (at 80 W) in all cases. The substrate temperatures were varied from room temperature to 500 °C. The background pressure was maintained below 1×10^{-4} Pa before introducing the working gases. The working pressure is kept at 1.0 Pa during depositing. Ar/N_2 with a ratio 2:1 was the working gas before the c-BN growth stage, and then was mixed with hydrogen ranging from 0 to 15% of working gases. These films were grown for 40 min–15 h respectively.

Fourier transform infrared spectroscopy (FTIR, Nicolet Avatar 370) was used to provide information about phase composition and film stress in transmission modes in the 400 cm^{-1}–4000 cm^{-1} range with a resolution of 4 cm^{-1}. The cubic content fraction was estimated by

$$\mathrm{cBN}\% = \frac{I_{1080\ \mathrm{cm}^{-1}}}{I_{1380\ \mathrm{cm}^{-1}} + I_{1080\ \mathrm{cm}^{-1}}} \times 100\%,$$

where is the peak intensity of cubic phase at 1080 cm^{-1}, and is the peak intensity of the hexagonal phase at 1380 cm^{-1}. All the films used to demonstrate the phase diagram of boron nitride were grown for 1 h, thus the influence of film thickness can be eliminated. These films were also analyzed by x-ray diffraction (XRD, LabX XRD-6000) measurements. The surface morphologies of the deposited films were studied by scanning electron microscopy (SEM, MAGELLAN 400) equipped with an electron beam, working at 10 kV.

3. Results and discussion

The parameters of BN films with varying hydrogen fraction and the substrate temperature are present in Fig. 1(a). The pure hexagonal phase exists in a low temperature region in spite of the hydrogen content varying. As the substrate temperature increases, the cubic phase forms gradually in the mediate region, beyond which a re-sputter region can be defined.

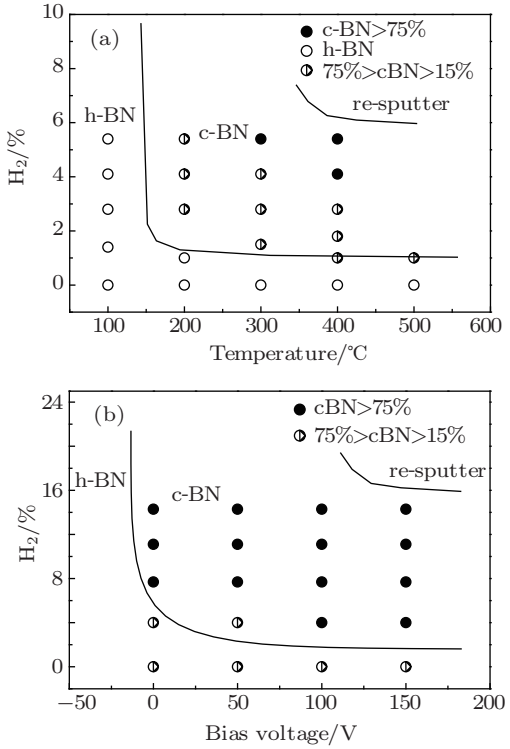


Fig. 1. Phase diagram of BN films, showing the variations of hydrogen content with substrate temperature (a), and bias voltage (b), respectively.

The threshold values of negative bias voltage can be determined for c-BN formation, h-BN formation, and re-sputter region, respectively. Generally a certain value of negative bias voltage is needed to enhance the ion bombardment for the nucleation of the cubic phase. Adding hydrogen is believed to etch sp^2 species more effectively than sp^3 ones.[38] Herein it is observed from Fig. 1(b) that the c-BN films form at lower bias voltage with the addition of hydrogen than those without the addition of hydrogen. Moreover, the c-BN content of the film deposited with additional H_2 in the working gasses is effectively increased. Furthermore, it is suggested that the introduction of hydrogen into reactive gases will diminish the

compressive stress induced by Ar ion bombardment, thereby being able to stabilize the films.[30]

In order to investigate the effect of growth parameters on the growth rate of c-BN films, the deposition rate is plotted versus the hydrogen content and the substrate temperature in Fig. 2. The hydrogen content is increased from 0 to 5.4% when keeping Ar:N_2 constant. While the substrate temperature is gradually varied from room temperature, 100 °C, 200 °C, 300 °C, 400 °C to 500 °C at each value of hydrogen content. Thus, a three-dimensional (3D) relationship between the deposition rate and the growth parameters is presented for the ease of direct understanding. It is observed that the film deposition rate increases as the substrate temperature increases, after reaching a maximum at about 300 °C, it reduces. From the discussion in the phase diagram of Fig. 1, it is known that the cubic phase nucleates only above 300 °C when the H_2 content is around 2%. When the substrate temperature is below 300 °C and the H_2 content is below 2%, the film consists of only hexagonal phases, which suggestes that the deposition rate of the h-BN film is greatly influenced by the substrate temperature in this region. The substrate temperature induced oriented *c* axis of h-BN plays a critical role for the deposition rate of the film. When adding hydrogen, the etching-off of h-BN can balance the deposition process. In the region of c-BN film consisting of mixture phases, the film deposition rate is co-determined by the interrelation of the formation of sp^2 and/or sp^3 phases and etching behavior induced by hydrogen. The maximum of deposition rate strongly depends on the equilibrium within these factors. While at each substrate temperature, the film deposition rate slowly decreases as the hydrogen gas increases. According to the phase diagram, the cubic phase increases in this region. Thus, it is probably due to the fact that the introduction of hydrogen will etch the deposited film partially while stabilizing the cubic phase.[39]

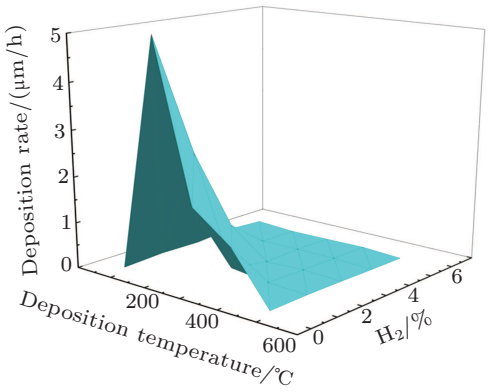


Fig. 2. (color online) Deposition rate as a function of deposition temperature and H_2 content.

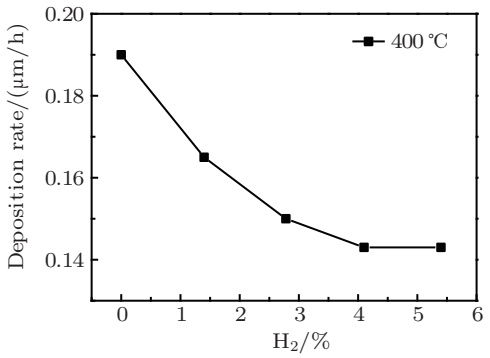


Fig. 3. Deposition rate as a function of H_2 content at 400 °C.

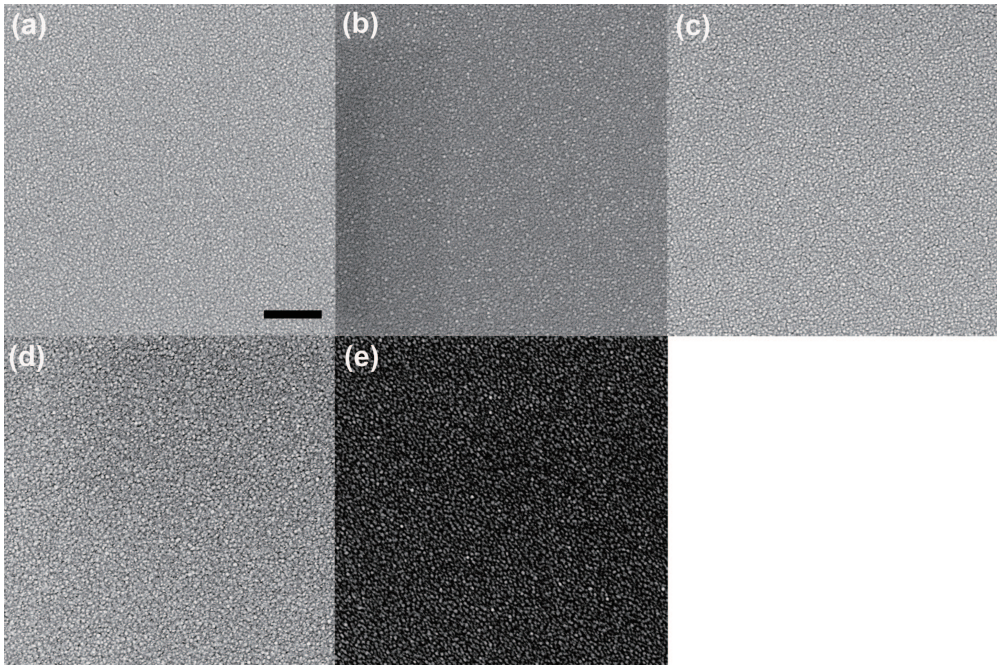


Fig. 4. SEM images of as-deposited c-BN films with thickness of 200 nm (a), 250 nm (b), 300 nm (c), 2.3 μm (d), 4.5 μm (e), respectively. Scale bar: 100 nm.

The deposition rate of a high c-BN content film grown at 400 °C is studied with hydrogen content increasing as displayed in Fig. 3. The hydrogen content gradually increases from 0 to 5.4%, while the bias voltage was maintained at −100 V for each deposition respectively. As the hydrogen content increases, the deposition rate significantly drops from 0.19 μm/h down to 0.14 μm/h. The involvement of hydrogen into reactive gas namely slows down the deposition rate. Meanwhile, it prefers to etch out the sp^2-bonded h-BN phase other than sp^3-bonded c-BN phase. The former is in favor of nucleating the cubic phase, while the latter can help to accumulate the cubic content in the context in the deposition time.

Figure 4 shows the surface morphologies of c-BN films with different thickness (thin films and thick films). The surface morphologies of all the c-BN films are smooth, continuous and dense without observable cracks nor pores in large-area scale no matter what the film thickness is. It is worth mentioning that several positions randomly localized on the surface are measured, and the results are similar. Statistically obtained average grain sizes of the films in Figs. 4(a)–4(e) are 8.9 nm, 11.1 nm, 12.8 nm, 13.3 nm, and 14.3 nm, respectively.

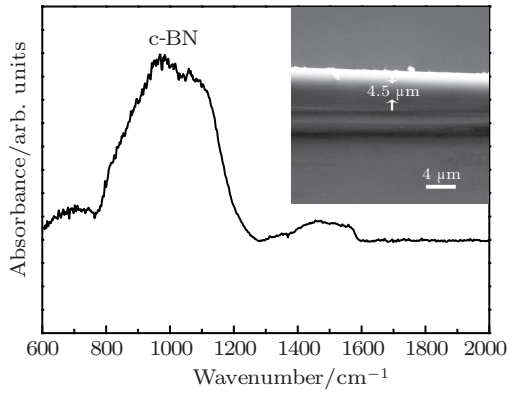


Fig. 5. FTIR spectra of the BN film deposited for 15 h. The insert shows the corresponding cross-section SEM image.

Figure 5 shows the FTIR spectrum for a typical c-BN thick film grown for 15 hours, and its cross-sectional SEM picture, showing that the c-BN film is ∼ 4.5 μm thick as indicated by the insert cross-section SEM image. A very strong FTIR absorption peak at about 1100 cm^{-1} is associated with the transverse optical (TO) mode of the sp^3-bonded BN structure (c-BN). The two minor peaks at 1380 cm^{-1} and 780 cm^{-1} are corresponding to the in-plane B–N stretching and out-of-plane B–N–B bending vibration in the sp^2-bonded h-BN phase. Besides, the peak located at 1505 cm^{-1} is probably attributed to the double phonon vibration in the c-BN phase. This is due to the fact that the IR beam is incident at 45° with respect to the sample surface, resulting in the enhancement of the LO mode. More than 95% of the cubic content can be estimated for this thick c-BN film by the equation previously mentioned.

Given the study above, a possible mechanism for the deposition of c-BN film in the gas atmosphere with additional H_2 is proposed. Figure 6 displays a surface parallel to the substrate in the c-BN growth region during the deposition, illustrating the etching effect of hydrogen. Hydrogen ions together with B^+ and N^+ in the reactive plasma form N–H^+, H^+ and/or B–H^+. Consider the fact that the bond energy of B–H^+ (340 kJ·mol^{-1}) is similar to that of N–H^+ (340 kJ·mol^{-1}), the possibilities of bond breaking for B–H^+ and N–H^+ are approximately the same. The etching of h-BN and/or c-BN surfaces by H^+ depends on the optimal window of the H_2 gas content.[38] At the high substrate temperatures at which the cubic phase is more likely to form, the H_2 content in the total working gas is a key to the equilibrium between the film formation and etching. According to previous reports,[7,31] the soft sp^2-bonded h-BN is more likely to be etched off than the hard sp^3-bonded cubic phase by H^+ ions. The decline of deposition rate due to the etching effect of additional hydrogen results in the accumulation of a cubic phase during the film growth at the equilibrium point.

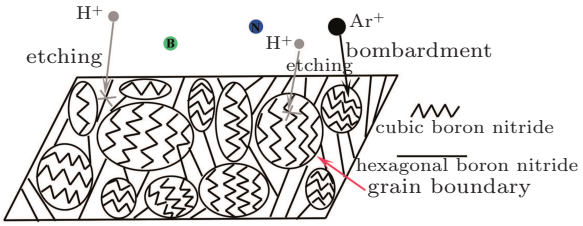


Fig. 6. (color online) Simplified diagram illustrating the etching effect of hydrogen during the growth of c-BN films.

4. Conclusions

In this work, we systematically investigate the growth conditions for thick c-BN films by adding additional hydrogen into Ar/N_2 mixture gases. Especially, the deposition rates versus hydrogen gas fraction for high-cubic-content BN films are investigated. The intentional involvement of hydrogen gas in the deposition process results in the decrease of the deposition rate by suppressing the growth of h-BN. By increasing the deposition time, 4.5 μm-thick c-BN films with over 95% cubic content can be achieved at a bias voltage of −80 V and substrate temperature of 400 °C. The present study offers a practical way to synthesize c-BN thick films for industry applications.

References

[1] Teii K and Matsumoto S 2015 *Thin Solid Films* **576** 50
[2] Schütze A, Bewilogua K, Lüthje H, Kouptsidis S and Jäger S 1995 *Surface and Coatings Technology* **74–75** 717
[3] Werbowy A, Szmidt J, Sokołowska A and Mitura S 2000 *Diamond and Related Materials* **9** 609
[4] Bello I, Chan C Y, Zhang W J, Chong Y M, Leung K M, Lee S T and Lifshitz Y 2005 *Diamond and Related Materials* **14** 1154

[5] Bewilogua K, Keunecke M, Weigel K and Wiemann E 2004 *Thin Solid Films* **469–470** 86
[6] Hangsheng Yang, Toyonobu C I and Yoshida 2002 *Thin Solid Films* **407** 67
[7] Mårlid B, K L and Carlsson J O 1999 *J. Phys. Chem.* **103** 7637
[8] Wang B, Qin Y, Yang J F and Ishizaki Kozo 2014 *Mater. Sci. Eng. A* **607** 490
[9] Deng J X, Qin Y, Kong L, Yang X L, Li T, Zhao W P and Yang P 2012 *Chin. Phys. B* **21** 047202
[10] Wang M E, Ma G J, Dong C and Gong S L 2014 *Chin. Phys. B* **23** 66805
[11] Zhang S J, Chen G H, Deng J X, Song X and Shao L X 2001 *Physics* **10** 0 (in Chinese)
[12] Song Z Z, Guo Y P, Zhang F Q and Chen G H 1995 *Physics* **5** 0 (in Chinese)
[13] Xu F, Yuen M F, He B, Wang C D, Zhao X R, Tang X L, Zuo D W and Zhang W J 2014 *Diamond and Related Materials* **49** 9
[14] Yang H S, Chen A and Qiu F 2011 *Diamond and Related Materials* **20** 1179
[15] Kian Ping Loh, N G M, Isao Sakaguchi, Takashi Taniguchi and Toshihiro Ando 1999 *Diamond and Related Materials* **8** 1296
[16] Mårlid B, Larsson K and Carlsson J O 2001 *Phys. Rev. B* **64** 184107
[17] Yang H S, Zhang J Y, Nie A M and Zhang X B 2008 *Chin. Phys. B* **17** 3453
[18] Weidner S, Geburt S, Milz S, Ye J, Ulrich S and Ronning C 2012 *Diamond and Related Materials* **22** 88
[19] Boyen H G, Widmayer P, Schwertberger D, Deyneka N and Ziemann P 2000 *Appl. Phys. Lett.* **76** 709
[20] Zhang W J and S M 2000 *Chem. Phys. Lett.* **330** 243
[21] Keunecke M, Wiemann E, Weigel K, Park S T and Bewilogua K 2006 *Thin Solid Films* **515** 967
[22] Zhang X W, Boyen H G, Deyneka N, Ziemann P, Banhart F and Schreck M 2013 *Nat. Mater.* **2** 312
[23] Ulrich S, Nold E, Sell K, Stüber M, Ye J and Ziebert C 2006 *Surface and Coatings Technology* **200** 6465
[24] Wang M E, Ma G J, Dong C and Gong S L 2014 *Chin. Phys. B* **23** 066805
[25] Yamamoto K 1, Keunecke U M and Bewilogua K 2000 *Thin Solid Films* **377–378** 331
[26] Schild D, Ulrich S, Ye J and Stüber M 2010 *Solid State Sciences* **12** 1903
[27] Ying J, Zhang X W, Fan Y M, Tan H R and Yin Z G 2010 *Diamond and Related Materials* **19** 1371
[28] Fan Y M, Zhang X W, You J B, Tan H R and Chen N F 2009 *Surface and Coatings Technology* **203** 1452
[29] Kim H S, Park J K, Lee W S and Baik Y J 2011 *Thin Solid Films* **519** 7871
[30] Ko J S, Park J K, Lee W S and Baik Y J 2013 *Surface and Coatings Technology* **223** 75
[31] Konyashin I, Khvostov V, Babaev V, Guseva M, Bill J and Aldinger F 1999 *Diamond and Related Materials* **8** 2053
[32] Park J K, Lee J H, Lee W S, Baik and Young J 2013 *Thin Solid Films* **549** 276
[33] Ko J S, Park J K, Lee W S, Huh J Y and Baik Y J 2013 *Thin Solid Films* **534** 380
[34] Bello I, Chong Y M, Leung K M, Chan C Y, Ma K L, Zhang W J, Lee S T and Layyous A 2005 *Diamond and Related Materials* **14** 1784
[35] Seiichiro Matsumoto and Zhang W J 2001 *Diamond and Related Materials* **10** 1868
[36] Konyashin I, Aldinger F, Babaev V, Khvostov V, Guseva M, Bregadze A, Baumgartner K M and uchle E Ra 1999 *Thin Solid Films* **355–356** 96
[37] Park J K, Ko J S and Baik Y J 2013 *Surface and Coatings Technology* **215** 104
[38] Zhang W J, Chan C Y, Meng X M, Fung M K, Bell I O, Lifshitz Y, Lee S T, and Jiang X 2005 *Angewandte Chemie* **44** 4749
[39] Han D, Li X B, Sun Y Y, Zhang S B, Xie S Y, Limpijumnong S, Chen Z G and Sun H B 2014 *Comput. Mater. Sci.* **82** 310